J Biol Inorg Chem (2006) 11: 433–444
DOI 10.1007/s00775-006-0090-0

ORIGINAL PAPER

Françoise Auchère · Sofia R. Pauleta
Pedro Tavares · Isabel Moura · José J. G. Moura

Kinetics studies of the superoxide-mediated electron transfer reactions between rubredoxin-type proteins and superoxide reductases

Received: 26 August 2005 / Accepted: 3 February 2006 / Published online: 17 March 2006

Abstract In this work we present a kinetic study of the superoxide-mediated electron transfer reactions between rubredoxin-type proteins and members of the three different classes of superoxide reductases (SORs). SORs from the sulfate-reducing bacteria *Desulfovibrio vulgaris* (*Dv*) and *D. gigas* (*Dg*) were chosen as prototypes of classes I and II, respectively, while SOR from the syphilis spyrochete *Treponema pallidum* (*Tp*) was representative of class III. Our results show evidence for different behaviors of SORs toward electron acceptance, with a trend to specificity for the electron donor and acceptor from the same organism. Comparison of the different k_{app} values, 176.9 ± 25.0 min^{-1} in the case of the *Tp*/*Tp* electron transfer, 31.8 ± 3.6 min^{-1} for the *Dg*/*Dg* electron transfer, and 6.9 ± 1.3 min^{-1} for *Dv*/*Dv*, could suggest an adaptation of the superoxide-mediated electron transfer efficiency to various environmental conditions. We also demonstrate that, in *Dg*, another iron–sulfur protein, a desulforedoxin, is able to transfer electrons to SOR more efficiently than rubredoxin, with a k_{app} value of 108.8 ± 12.0 min^{-1}, and was then assigned as the potential physiological electron donor in this organism.

Keywords Superoxide reductase · Rubredoxin · Oxidative stress · Iron–sulfur protein · Electron transfer

Abbreviations *Dg*: *Desulfovibrio gigas* · *Dv*: *Desulfovibrio vulgaris* · SOD: Superoxide dismutase · SOR: Superoxide reductase · *Tp*: *Treponema pallidum* · Tris: Tris(hydroxymethyl)aminomethane

Introduction

Superoxide reductases (SORs), non-heme iron enzymes initially found in sulfate-reducing bacteria, play a fundamental role in the defense of microorganisms against oxidative stress, by catalyzing the monovalent reduction of the superoxide anion, rather than the dismutation, according to Eq. 1 [1–11]:

$$O_2^{\bullet -} + 2H^+ + e^- \rightarrow H_2O_2. \quad (1)$$

These enzymes, present in most known anaerobes, including strictly anaerobes and microaerophiles, have been classified into three different classes, distinguished by the presence or absence of an N-terminal domain (Fig. 1) [12]. SORs from the three classes share a conserved C-terminal domain of approximately 100 amino acids that accommodates a single iron-containing active site coordinated by four equatorial histidine nitrogen atoms (three ε and one δ) and an axial cysteinyl sulfur atom, designated as center II [3, 9, 13–15].

Class I SORs, also called desulfoferrodoxins, have been isolated from the sulfate-reducing bacteria *Desulfovibrio vulgaris* (*Dv*) [9, 16–18], *Desulfovibrio desulfuricans* [9, 11], and *Desulfoarculus barsii* [19, 20]. These SORs bind two iron atoms in two distinct centers (Fig. 1). In addition to the C-terminal domain, which contains the active site called center II, class I SOR also has an iron in the N-terminal domain (center I), which is coordinated by four conserved cysteines residues in a distorted tetrahedral coordination. This center is homologous to that present in desulforedoxin, an

Electronic Supplementary Material Supplementary material is available for this article at http://dx.doi.org/10.1007/s00775-006-0090-0 and is accessible for authorized users.

F. Auchère · S. R. Pauleta · P. Tavares · I. Moura
J. J. G. Moura (✉)
REQUIMTE—Centro de Química Fina e Biotecnologia, Departamento de Química, Faculdade de Ciências e Tecnologia, Universidade Nova de Lisboa, 2829-516, Caparica, Portugal
E-mail: jose.moura@dq.fct.unl.pt
Tel.: +351-21-2948382
Fax: +351-21-2948550

Present address: F. Auchère
Laboratoire d'Ingénierie des Protéines et Contrôle Métabolique, Dépt. de Biologie des Génomes, Institut Jacques Monod (UMR 7592 CNRS—Universités Paris 6 et 7), 2 Place Jussieu, 75251, Paris Cedex 05, France
E-mail: aucherefrancoise@yahoo.com
Tel.: +33-1-44278170
Fax: +33-1-44275716

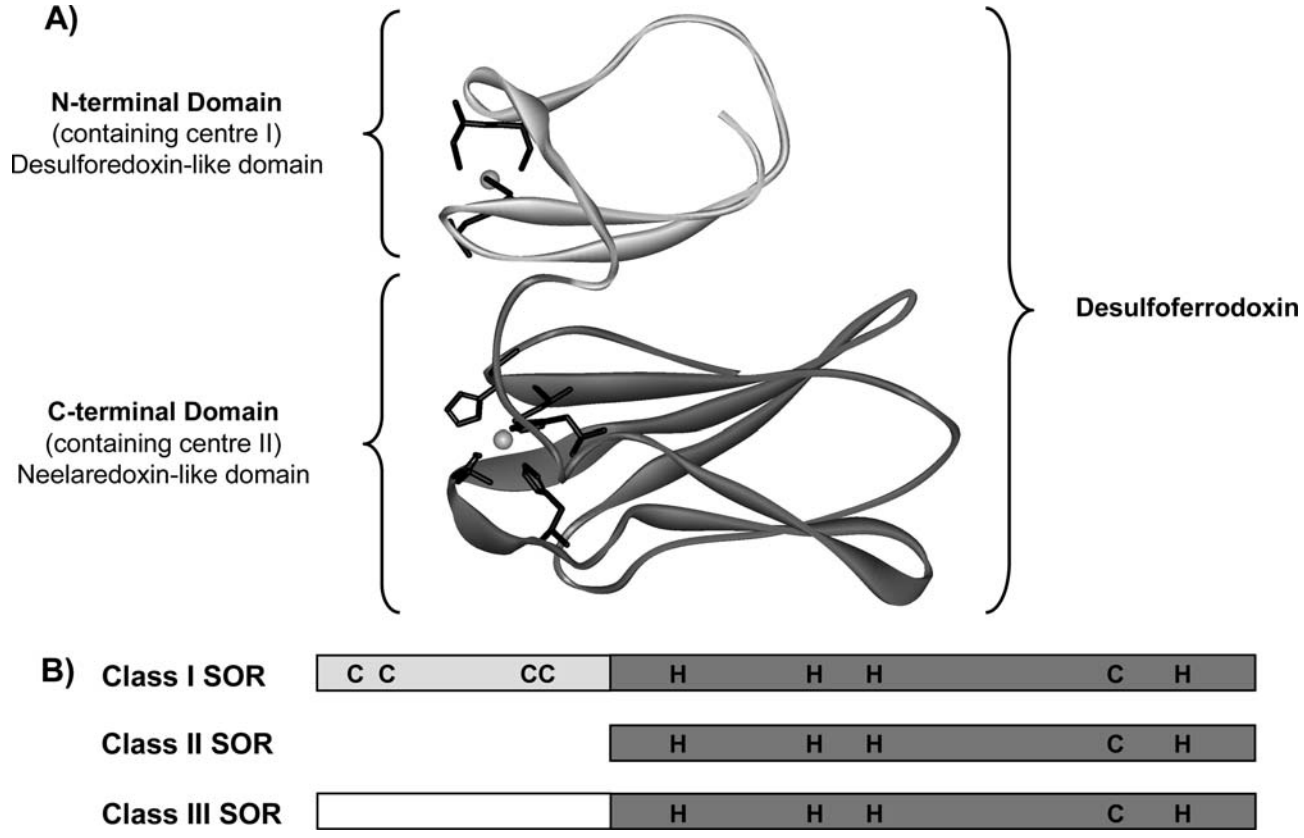

Fig. 1 **a** Model structure of *Desulfovibrio vulgaris* (*Dv*) superoxide reductase (*SOR*), a representative of class I SOR. The protein is shown as a backbone with the iron centers *space-filled* and the ligands of the iron centers as *sticks*. The N-terminal domain is colored *light gray* and the C-terminal domain *dark gray*. The model was obtained using DeepView (Swiss-PdbViewer) and the structure of *D. desulfuricans* 27774 SOR (1DFX.pdb), another representative of class I SOR [14, 61]. These two enzymes have a 77.4% sequence identity. **b** Schematic alignment of the three classes of SOR. This representation is based on the amino acid sequence alignment of different SORs (data not shown). The residues shown are the ligands of the iron centers and the color scheme is as in **a**

iron–sulfur protein isolated from *Desulfovibrio gigas* (*Dg*) [21–23].

Class II SORs lack the N-terminal desulforedoxin-like domain and are historically referred to as neelaredoxins, in reference to the prototype isolated from *Dg* [3, 24]. SORs from *Pyrococcus furiosus* [4, 15], *Archeoglobus fulgidus* [1, 25], or *Methanococcus Janaschii* [26] also belong to this family.

The SOR from *Treponema pallidum* (*Tp*), the syphilis spirochete, classified as a microaerophile, is an example of class III SORs, and has an extended non-iron N-terminal domain of unknown function (Fig. 1) [5, 8, 27].

Only the reduced form of the iron-containing active site of SORs is able to react with the substrate, the superoxide anion $O_2^{\bullet -}$, with a virtually diffusion controlled rate of 10^9 M^{-1} s^{-1}, leading to the formation of the ferric state of the enzyme. Therefore, the presence of an electron donor is necessary to regenerate the ferrous active form and complete the catalytic cycle of the enzyme [10, 19, 28–31]. Recently, several groups, including ours, have clearly established rubredoxin as the proximal electron donor to SORs in the case of *Tp*, *Dv*, *P. furiosus*, and *A. fulgidus* [4, 32–36].

Rubredoxins, previously isolated from *Clostridium pasteurianum* [37] and found in a variety of anaerobic and aerobic bacteria and archea, are small, soluble iron–sulfur proteins (45–54 amino acids), which feature an iron atom coordinated in a tetrahedral geometry to the four cysteinyl sulfur atoms of four conserved cysteine residues, with a common motif of two pairs of Cys–XX–Cys and a molecular weight ranging from 5,000 to 6,000 [37–42]. In anaerobes, it is often observed that the genes encoding rubredoxin occur in the same operon or cluster as SORs, the gene for SOR usually being located some base pairs downstream of the gene-encoding rubredoxin [1, 26, 43–45]. Moreover, a coordinated expression of the genes has also been described in some organisms, such as *Dv* and *Desulfoarculus barsii* [16, 43, 44].

The first kinetics data showing an electron transfer from rubredoxin to *Dv* SOR were for an NADPH superoxide oxidoreductase artificial cycle [33, 35, 36, 46]. Last year, we showed, using a different assay, kinetics evidence for a superoxide-mediated electron transfer from *Tp* (and *Dv*) rubredoxins to *Tp* SOR, and calculated the kinetics parameters of the electron transfer reaction [32]. Now, we have extended this study and present kinetics data of the reactions between members of the three different classes of SORs and rubredoxin-like proteins from the same organisms: *Dv* SOR was chosen as the prototype of class I, *Dg* SOR as that of

class II, and *Tp* SOR as that of class III. Our results show evidence for a superoxide-mediated electron transfer between rubredoxins and SORs from the different classes, and establish desulforedoxin, a rubredoxin-like protein, as the physiological electron donor to *Dg* SOR. Moreover, analysis of the different rate constants suggests that the efficiency of the superoxide-mediated electron transfer reactions may be related to an adaptation of the SOR activity to environmental conditions.

Materials and methods

Chemicals

Bovine Cu,Zn superoxide dismutase (SOD), bovine milk xanthine oxidase, bovine liver catalase, xanthine, horse heart cytochrome *c*, Luria–Bertani medium, ampicillin, and isopropyl-β-D-thiogalactopyranoside were purchased from Sigma Chemical Co. (St Louis, MO, USA). Sodium dithionite ($Na_2S_2O_4$), sodium hexachloroiridate (Na_2IrCl_6), and potassium ferricyanide ($K_3[Fe(CN)_6]$) were obtained from Aldrich Chemical Co. All buffer salts were from Merck (Mannheim, Germany). Competent *Escherichia coli* BL21(DE3) cells were from Novagen (Madison, WI, USA). All reagents and buffers were of the highest grade commercially available.

Spectroscopic measurements

Absorbance spectra, repetitive scans, and kinetics absorbance measurements were performed at 20 °C with a Hewlett-Packard 8452 A diode-array spectrophotometer, interfaced with a computer allowing the collection of data. Manipulation and analysis of data were then performed using the Kaleidagraph 3.5 software.

Overexpression and purification of recombinant *Dv* (strain Hildenborough) rubredoxin and SOR (class I)

The *Dv* rubredoxin was overexpressed and purified to homogeneity following a protocol adapted from that published for the purification of *Dg* desulforedoxin [47], and already described in Ref. [32]. *Dv* SOR was overexpressed and purified to homogeneity following the previously published procedures [2].

Overexpression and purification of recombinant *Dg* rubredoxin, desulforedoxin, and SOR (class II)

The *Dg* rubredoxin gene was cloned (Pauleta et al., unpublished results) and the purification followed a modified procedure of that in Ref. [47]. *Dg* desulforedoxin was overexpressed and purified to homogeneity following the protocol published in Ref. [47]. A typical purification process involved anion exchange [(diethylamino)ethyl-Sepharose, Pharmacia] and gel filtration (Sephadex G75, Amersham Biosciences) chromatographies of crude extracts obtained from *E. coli* cells overexpressing the desulforedoxin gene. *Dg* SOR was cloned and overexpressed in our laboratory, and was purified to homogeneity using a protocol identical to that used for the purification of *Tp* SOR [5].

Overexpression and purification of recombinant *Tp* rubredoxin and SOR (class III)

The *Tp* rubredoxin was cloned and overexpressed in our laboratory and then purified to homogeneity following the protocol published in Ref. [32]. After overexpression of the gene in *E. coli* cells, a typical purification process involved a combination of affinity (Ni nitrilotriacetic acid resin, BioRad) and anion-exchange (MonoQ-HR5/5 resin, Pharmacia) chromatographies. Pure fractions were pooled and concentrated using an Amicon unit cell, equipped with a YM3 membrane, before being used for kinetics experiments. *Tp* SOR was cloned, overexpressed, and purified to homogeneity using a combination of anion-exchange and gel filtration chromatography, as previously described in Ref. [5].

Reduction of *Tp*, *Dg*, and *Dv* rubredoxins, and of *Dg* desulforedoxin

Reduction of recombinant rubredoxins and desulforedoxin was accomplished by careful spectrophotometric titration with freshly prepared anaerobic solutions of sodium dithionite ($E_{midpoint} = -420$ mV), following the procedure described in Ref. [32]. Sodium dithionite stock solution of 100 mM was first prepared in 1 M tris(hydroxymethyl)aminomethane (Tris)–HCl (pH 9.0) under argon, and then dilute solutions were made and used within a few hours. The concentrations of all the dithionite solutions were standardized at 420 nm ($\varepsilon = 1.02\ mM^{-1}\ cm^{-1}$) [48]. Addition of sodium dithionite resulted in a decrease of the 490-nm feature (or of the 502-nm feature in the case of desulforedoxin) of the spectrum, characteristic of the ferric form of the protein. The titrations were conducted until the spectrum of the fully reduced rubredoxin (or desulforedoxin) was obtained, i.e., until disappearance of the 490-nm (or 502-nm) absorbance, but before the absorption of excess dithionite was observed. Proteins concentrations were determined using the published molecular absorption coefficients of the oxidized forms, $\varepsilon_{490\ nm} = 6.9\ mM^{-1}\ cm^{-1}$ for *Dv* rubredoxin [33, 49], $\varepsilon_{490\ nm} = 6.9\ mM^{-1}\ cm^{-1}$ for *Tp* rubredoxin [32], $\varepsilon_{490\ nm} = 6.6\ mM^{-1}\ cm^{-1}$ for *Dg* rubredoxin [50], and $\varepsilon_{502\ nm} = 7\ mM^{-1}\ cm^{-1}$ for *Dg* desulforedoxin [21].

Oxidation of class I *Dv* SOR

A sample of the as-isolated pink desulfoferrodoxin (oxidized center I and reduced center II) was treated with a slight excess of sodium hexachloroiridate in 50 mM Tris–HCl pH 7.8, which resulted in the oxidation of center II and the formation of the gray (fully oxidized) form of the protein. The differential spectra between the gray and pink forms of SOR revealed the appearance of a new feature at 635 nm, characteristic of the oxidized center II of the protein ($\varepsilon_{635\ nm} = 1.8\ mM^{-1}\ cm^{-1}$) [2]. Full oxidation of SOR was followed by the removal of the excess of oxidant by passage of the sample over an NAP-25 column (Amersham Biosciences) equilibrated with 50 mM Tris–HCl, pH 7.8.

Oxidation of class II *Dg* and class III *Tp* SORs

Oxidized SOR was obtained by treating a sample of the purified protein with a slight excess of sodium hexachloroiridate with 50 mM Tris–HCl, pH 7.8, followed by the removal of the excess of oxidant by passage of the sample over an NAP-25 column equilibrated with 50 mM Tris–HCl, pH 7.8. Addition of sodium hexachloroiridate resulted in an increase of the absorbance at 656 nm, characteristic of the ferric form of the protein. A slight excess of sodium hexachloroiridate was defined as the amount that no longer produced further increase in the absorbance at 656 nm. Concentrations of the oxidized proteins were calculated using the molecular absorption coefficient of the feature of oxidized SOR at 656 nm, $\varepsilon = 2.6\ mM^{-1}\ cm^{-1}$ for *Tp* SOR and $\varepsilon = 2.06\ mM^{-1}\ cm^{-1}$ for *Dg* SOR [5, 45]. For all the assays described, we verified that sodium hexachloroiridate, which does not bind to the enzyme, was not interfering in the reaction between rubredoxin and SOR.

Treatment of *Tp* SOR with potassium ferricyanide

A 100-μM sample of the purified protein was treated with various concentrations of potassium ferricyanide ($K_3[Fe(CN)_6]$) in 50 mM Tris–HCl, pH 7.8, resulting in an increase of the absorbance at 656 nm, characteristic of the ferric form of the protein, and the appearance of a new band in the near-IR around 1,020 nm, characteristic of the ferrocyanide adduct described in Ref. [51]. The $K_3[Fe(CN)]_6$ excess was removed by passage of the sample over an NAP-25 column equilibrated with 50 mM Tris–HCl, pH 7.8. Concentrations of the $K_3[Fe(CN)_6]$-treated enzyme were calculated using the molecular absorption coefficient of the feature of oxidized SOR at 656 nm, $\varepsilon = 2.6\ mM^{-1}\ cm^{-1}$ for *Tp* SOR [5, 45], and the concentration used in the kinetics assays was of 0.03 μM.

Superoxide-mediated electron transfer experiments between rubredoxins and SORs (“classical” assay)

The assays were performed aerobically at 20 °C in a 1-ml quartz cuvette containing approximately 12 μM rubredoxin in 50 mM phosphate buffer, pH 7.8, chosen to allow the maximum electron transfer rates under our experimental conditions, as previously described in Ref. [32]. After addition of sodium dithionite, reduction of rubredoxin was reflected by a decrease in the absorbance at 490 nm. After approximately 1 min, xanthine (0.5 mM) and xanthine oxidase (0.058 U ml^{-1}) were added to the cuvette, in order to generate a continuous flux of superoxide of around 14 μM min^{-1}. After addition of xanthine/xanthine oxidase, a slow reoxidation of rubredoxin was observed, but was greatly accelerated by the addition of a catalytic amount of oxidized SOR. The specific rubredoxin oxidation rate was derived by comparing the initial rates of rubredoxin oxidation before and upon addition of SOR. All data points in the figures and the values listed represent averages of triplicates or more determinations, and statistic calculations (Student’s law) were used to determine the different k_{app} values.

The flux of superoxide was calibrated before and after every experiment by measuring the rate of reduction of a saturating 10 μM horse heart cytochrome *c* at 550 nm ($\varepsilon = 21\ mM^{-1}\ cm^{-1}$), in the presence of the same concentration of xanthine/xanthine oxidase as in the assay mixture [52]. These experiments were performed as described earlier, using 12 μM *Dv* rubredoxin and 0.12 μM *Tp* SOR, in the presence of 0.058 U ml^{-1} xanthine oxidase and different concentrations of xanthine, varying from 0.01 to 0.75 mM, and we determined that, with this concentration of 0.5 mM xanthine, the steady-state conditions were achieved (see “Results”).

Moreover, for all experiments, 150 U ml^{-1} bovine catalase was added to the reaction mixture, in order to remove H_2O_2, which is not only a product of the SOR reaction, but is also a by-product of the xanthine/xanthine oxidase superoxide-generating system [52, 53].

Superoxide-mediated electron transfer experiments between *Dg* desulforedoxin and SOR (modified assay)

To study this electron transfer reaction, we had to develop a modified procedure of our “classical” assay described earlier and in Ref. [32]. These assays were performed aerobically at 20 °C in a 1-ml quartz cuvette containing approximately 9 μM desulforedoxin in 50 mM phosphate buffer, pH 7.8. After addition of sodium dithionite, reduction of desulforedoxin was reflected by a decrease in the absorbance at 502 nm. After approximately 1 min, a catalytic amount of oxidized SOR was added, resulting in no reoxidation of desulforedoxin. After a further 1 min of incubation, xanthine (0.5 mM) and xanthine oxidase (0.058 U ml^{-1}) were added to the cuvette, resulting in the reoxidation of

desulforedoxin, as shown in the kinetics trace of Fig. 6, and the specific desulforedoxin oxidation rate was derived from the linear part of the reoxidation kinetics. In order to validate this modified assay, electron transfer reactions between *Dg* rubredoxin and *Dg* SOR were performed using the two experimental procedures. As expected, the rubredoxin oxidation rate observed using this procedure was equal to the difference of rubredoxin oxidation rates, before and upon addition of the xanthine/xanthine oxidase system, determined using our classical assay.

Results

As previously described in Ref. [32], a classical kinetics assay involved the reduction of rubredoxin by addition of an excess of sodium dithionite, followed by the addition of the xanthine/xanthine oxidase system, in order to generate a controlled steady-state concentration of the superoxide anion. Addition of xanthine/xanthine oxidase resulted in a slow reoxidation of *Dv* rubredoxin, *Dg* rubredoxin, and *Tp* rubredoxin, with respective rates of 2.2 ± 0.7, 1.7 ± 0.7, and 1.5 ± 0.5 μM min^{-1}, reoxidation which has been attributed to a reaction with superoxide [4, 32]. Further addition of catalytic amounts of SOR resulted in an acceleration of this oxidation rate, in a SOR concentration-dependent manner. In order to prevent any involvement of H_2O_2 in our assay, bovine catalase was also added to the reaction mixture, in a relatively high concentration (150 U ml^{-1}) [33, 46].

The rate of rubredoxin oxidation was then calculated from the difference between the initial rates of rubredoxin oxidation before and upon addition of various amounts of SOR, as previously reported in Ref. [32].

To test the effect of the superoxide concentration on the electron transfer kinetics, the assays were performed in the presence of different concentrations of xanthine, varying from 0.1 to 0.75 mM, as described in the "Materials and methods" (classical assay). The results obtained (Fig. 2) show that the superoxide-mediated *Tp* rubredoxin oxidation rate presents a saturation behavior related to the superoxide concentration, and reaches a plateau when a continuous flux of 5 μM superoxide is generated by the xanthine/xanthine oxidase system. These data allowed the estimation of an apparent K_m value of 0.8 μM. In view of these results, the concentration of 0.5 mM xanthine used in all kinetics assays was chosen so as to generate around 14 μM superoxide, corresponding to saturating conditions.

Moreover, for all the rubredoxin/SOR studies presented here, electron transfer experiments were performed in the presence of different concentrations of rubredoxin (4–20 μM) with no change in the rubredoxin oxidation rates (data presented in the supplementary material). Therefore, we assume that a rubredoxin concentration around 12 μM, which was the concentration used in our comparative assays, reflected the saturating conditions in rubredoxin.

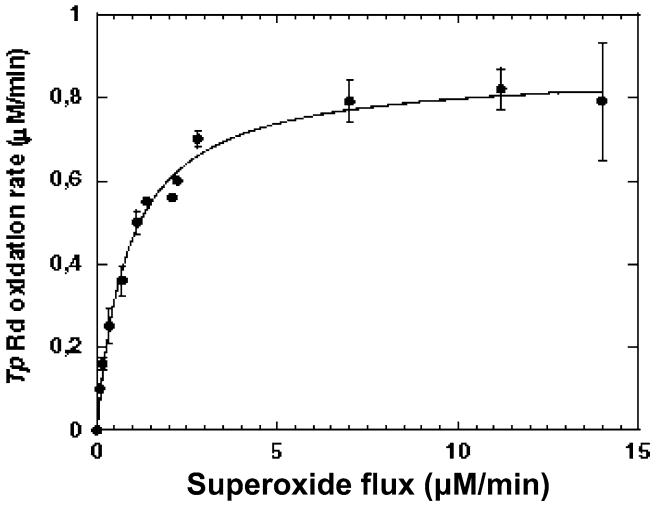

Fig. 2 Dependency of *Treponema pallidum* (*Tp*) rubredoxin oxidation rate as a function of the superoxide flux generated by the xanthine/xanthine oxidase system. Experiments were performed as described in the "Materials and methods," using 12 μM *Dv* rubredoxin and 0.12 μM *Tp* SOR, in the presence of 0.058 U ml^{-1} xanthine oxidase and different concentrations of xanthine, varying from 0.01 to 0.75 mM. The flux of superoxide was calibrated before and after every experiment by measuring the rate of reduction of a saturating 10 μM horse heart cytochrome *c* at 550 nm ($\varepsilon = 21$ mM^{-1} cm^{-1}), in the presence of the same concentration of xanthine/xanthine oxidase as in the assay mixture [51]. All data points in the figure represent averages of at least three determinations. Where not visible in the figure, the range bars lie within the diameter of the symbol

In view of these experiments, the concentration of both superoxide and rubredoxin could be considered constant under our experimental procedure; therefore, we can apply the following kinetics model, with *v* being the rubredoxin oxidation rate:

$$v = k_{app}[\mathrm{SOR}]. \quad (2)$$

Specificity of the superoxide-mediated electron transfer reaction towards active forms of SORs

In order to determine the specificity of the superoxide-mediated electron transfer reaction towards SOR, we performed the classical assay, described in the "Materials and methods," replacing SOR by SOD. In one of the experiments SOD was added at the same time as the superoxide-generating system, in a concentration of 0.05 μM, which is able to fully trap the superoxide, as shown in Fig. 3, trace d. In another experiment, SOD was added in place of SOR, in equivalent amounts (0.05 μM), and the complete inhibition of the rubredoxin oxidation was observed, confirming the specificity of the electron donation from rubredoxin to SOR (Fig. 3, trace c). Addition of both SOD and SOR (Fig. 3, trace b) resulted in an inhibition of the reaction,

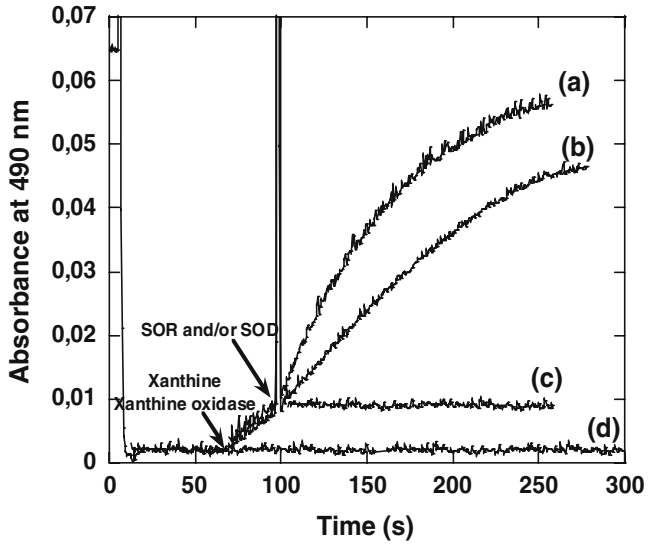

Fig. 3 Effect of addition of superoxide dismutase (*SOD*) at various stages of the superoxide-mediated electron transfer reaction. Experiments were performed as described in the "Materials and methods." *Tp* rubredoxin oxidation after addition of *a* 0.05 μM *Tp* SOR, *b* equivalent amounts of *Tp* SOR and bovine SOD (0.05 μM), *c* 0.05 μM bovine SOD, and *d* 0.05 μM bovine SOD at the same time as the superoxide-generating system

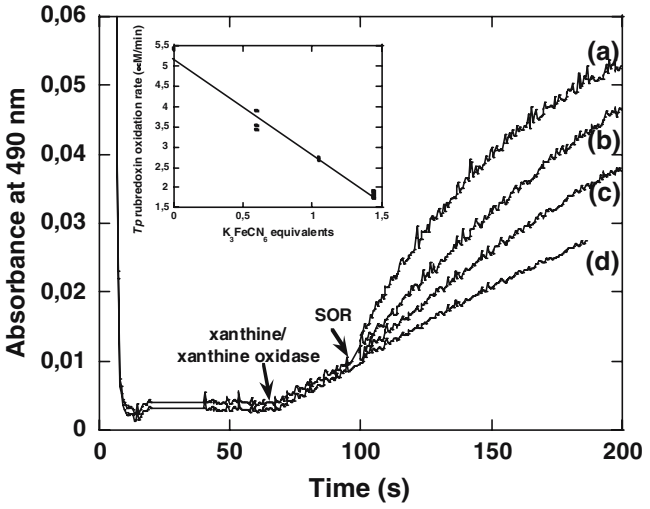

Fig. 4 Kinetics traces of the superoxide-mediated electron transfer between *Tp* rubredoxin and $K_3[Fe(CN)_6]$-pretreated *Tp* SOR. Experiments were performed aerobically at 20 °C in a 1-ml quartz cuvette containing 10 μM *Tp* rubredoxin in 50 mM phosphate buffer, pH 7.8, as previously described in the "Materials and methods." Addition of xanthine/xanthine oxidase resulted in a slow oxidation of rubredoxin, with a rate of 1.9 μM min^{-1}, which was accelerated by the addition of *a* 0.03 μM *Tp* SOR, and the same concentration of *Tp* SOR pretreated with *b* 0.6 equiv K_3FeCN_6, *c* 1.05 equiv K_3FeCN_6, and *d* 1.5 equiv K_3FeCN_6. *Insert* Rubredoxin oxidation rates as a function of the number of K_3FeCN_6 equivalents used in the pretreatment of *Tp* SOR

by comparison of the rate of rubredoxin oxidation when only SOR was added (Fig. 3, trace a). These results confirm that SOD cannot catalyze the electron transfer reaction, but it is able to compete with SOR for reaction with the superoxide anion.

The effect of treating SOR with potassium ferricyanide was also studied. The reaction of SORs with potassium ferricyanide has been described to produce a ferrocyanide adduct with the protein [32], leading to the inaccessibility of the superoxide anion to the hexacoordinated iron atom. Figure 4 shows that treatment of SOR with various equivalents of potassium ferricyanide resulted in an inhibition of the superoxide-mediated rubredoxin oxidation, in a $K_3[Fe(CN)_6]$-dependent manner. Moreover, inhibition of the electron transfer reaction was directly proportional to the amount of ferricyanide added, as shown in insert of Fig. 4, and around 1.5 equiv of ferricyanide was able to fully inhibit the reaction.

Altogether, these results show that the hexacoordinated ferrocyanide adduct of SOR was, in our conditions, unable to participate in a superoxide-mediated electron transfer reaction with rubredoxin, and suggest that our assay could be used, in vitro, to reveal a SOR activity.

Superoxide-mediated electron transfer between rubredoxins and SORs from the three different classes

Extensive kinetics studies of the superoxide-mediated electron transfer reactions between rubredoxins and SORs from the three different classes were performed, using the classical kinetics assay described earlier. *Dv* SOR (class I, contains two iron centers), *Dg* SOR (class II, does not contain an N-terminal domain), and *Tp* SOR (class III, contains a non-iron N-terminal domain) (Fig. 1) were chosen for these experiments.

SORs containing a single iron center: class II and class III SORs

The plots of the oxidation rates of the different rubredoxins as a function of the class II *Dg* SOR concentration are presented in Fig. 5. For the three reactions presented in this figure, the initial rubredoxin oxidation rate was found to be proportional to the amount of SOR added to the reaction mixture, and revealed the existence of a direct electron transfer between the three rubredoxins and the *Dg* SOR. Linear regressions of the three curves, shown in Fig. 5, allowed the calculation of the specific activities (micromoles per liter of oxidized rubredoxin per minute per micromole per liter of *Dg* SOR), which, in agreement with Eq. 2 and Ref. [32], reflect the k_{app} value of the electron transfer reaction, and thus the ability of the three different rubredoxins to give electrons to *Dg* SOR.

Although all three rubredoxins were able to transfer electrons to *Dg* SOR, a closer analysis of the curves of Fig. 5 revealed that *Dg* rubredoxin is the best electron donor to *Dg* SOR, with a k_{app} value of 31.8 ± 3.6 min^{-1}

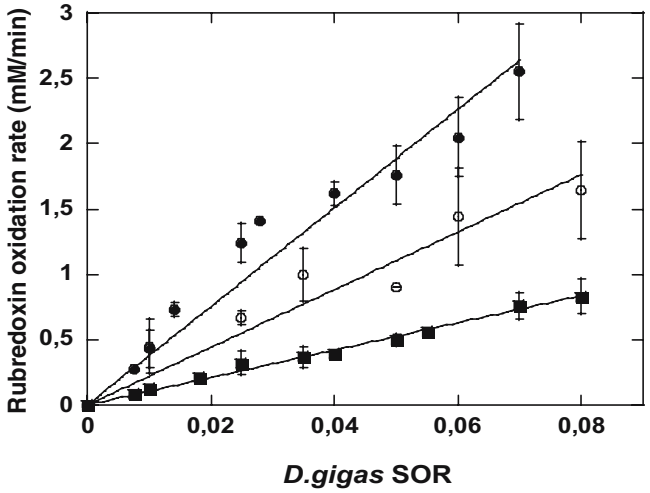

Fig. 5 Comparison of superoxide-mediated electron transfer reactions from *D. gigas* (*Dg*) rubredoxin (*filled circles*), *Dv* rubredoxin (*open circles*), and *Tp* rubredoxin (*squares*) to *Dg* SOR. Experiments were performed aerobically at 20 °C in a 1-ml quartz cuvette containing 12 μM rubredoxin in 50 mM phosphate buffer, pH 7.8, with the enzyme being added last, as described in the "Materials and methods." Rubredoxin initial oxidation rates were measured in the presence of different concentrations of *Dg* SOR, and the k_{app} values of the superoxide-mediated electron transfer reactions, shown in Table 1, were determined from the linear regression of the plots, using the statistic calculations of Student's law. All data points in the figure represent averages of at least three determinations. Where not visible in the figure, the range bars lie within the diameter of the symbol

(Fig. 5, filled circles), whereas *Dv* (Fig. 5, open circles) and *Tp* (Fig. 5, squares) rubredoxins are less efficient towards electron donation to *Dg* SOR, with respective activities of 18.4 ± 5.0 and 10.2 ± 1.0 min^{-1} (Table 1). These results suggest a trend for specificity between rubredoxin and *Dg* SOR, in regard to the electron transfer reaction, in favor of a reaction implicating the electron donor and acceptor from the same organism.

Similar experiments were performed for *Tp* SOR (class III) and the three rubredoxins (Table 1). These results reveal a different behavior of *Dg* and *Tp* rubredoxins and their homolog SORs towards electron donation and acceptance. Indeed, *Dg* SOR is shown to preferentially receive electrons from *Dg* rubredoxin, as described in Fig. 5, and *Tp* SOR is able to accept electrons from *Dg* rubredoxin, as efficiently as from *Tp* rubredoxin, with respective k_{app} values of 213.4 ± 38.4 and 176.9 ± 25.0 min^{-1} (Table 1). *Tp* SOR was even able to accept electrons from desulforedoxin, another rubredoxin-type protein, with a k_{app} value of 156.0 ± 19.0 min^{-1} (Table 1).

Table 1 Apparent rate constants (k_{app}) of superoxide-mediated electron transfer reactions between rubredoxin-like proteins and superoxide reductases (SORs) from *Treponema pallidum* and *Desulfovibrio gigas* (classes II and III SORs)

	Tp SOR (class III) (min^{-1})	*Dg* SOR (class II) (min^{-1})
Tp rubredoxin	176.9 ± 25.0[a]	10.2 ± 1.0
Dv rubredoxin	4.3 ± 1.0[a]	18.4 ± 5.0
Dg rubredoxin	213.4 ± 38.4	31.8 ± 3.6
Dg desulforedoxin	156.0 ± 19.0	108.8 ± 12.0

Assays were performed as described in the "Materials and methods." All data points and values listed represent averages of triplicates or more determinations. The k_{app} values were calculated using the linear part of the rubredoxin oxidation rate versus the concentration of SOR (see Fig. 3 and Ref. [32]), and applying statistic calculations of Student's law

Dg Desulfovibrio gigas, *Dv Desulfovibrio vulgaris*, *Tp Treponema pallidum*

[a]Calculated using a combination of the values published in Ref. [1] and new experimental data

SOR containing two iron centers: class I SOR

Apparent superoxide-mediated electron transfer rates between rubredoxins and *Dv* SOR are presented in Table 2. These values reveal that *Dv* SOR was able to receive electrons from the three types of rubredoxins. However, closer analysis of the data shows that the reaction was more efficient when the reaction involved *Dv* rubredoxin, which should be its physiological electron donor.

In addition to the neelaredoxin-like active site, the so-called center II, class I *Dv* SOR also presents an iron-containing N-terminal domain (center I) (Fig. 1), in which the iron is coordinated in a distorted tetrahedral geometry similar to that found in desulforedoxin, as previously described [9, 11, 16, 21, 22]. It has been proposed that this center could play a role in the electron transfer pathway [2, 16, 45].

To test this hypothesis, the kinetics assays were performed in the presence of both pink (oxidized center I and reduced center II) and gray (fully oxidized) forms of *Dv* SOR. Table 2 shows that both pink and gray forms of *Dv* SOR were able to receive electrons from *Dv* rubredoxin, but surprisingly, the pink form of *Dv* SOR seems to be a better electron acceptor than the fully oxidized gray form of *Dv* SOR.

Table 2 Apparent rate constants (k_{app}) of superoxide-mediated electron transfer reactions between rubredoxins from various organisms and two forms of *D. vulgaris* SOR (pink and gray forms)

	Dv SOR (class I) (pink form) (min^{-1})	*Dv* SOR (class I) (gray form) (min^{-1})
Tp rubredoxin	2.9 ± 0.3	1.3 ± 0.2
Dv rubredoxin	11.4 ± 1.0	6.9 ± 1.3
Dg rubredoxin	8.3 ± 1.1	4.4 ± 0.8

Assays were performed as described in the "Materials and methods." All data points and values listed represent averages of triplicates or more determinations. The k_{app} values were calculated using the linear part of the rubredoxin oxidation rate versus the concentration of SOR (see Fig. 3 and Ref. [32]), and applying statistic calculations of Student's law

Evidence for desulforedoxin as the potential physiological electron donor to class II *Dg* SOR

The results presented in Table 1 show an apparent good specificity of *Dg* rubredoxin as the physiological electron donor to *Dg* SOR. However, in addition to rubredoxin, *Dg* also contains the so-called desulforedoxin, a small iron–sulfur homodimeric protein, in which the iron atom is coordinated to four cysteines in a distorted tetrahedral environment [21, 22, 54]. The presence of both rubredoxin and desulforedoxin in the same organism has suggested that rubredoxin might not be the unique electron donor to *Dg* SOR, but, to our knowledge, no evidence for a redox partnership between desulforedoxin and SOR has been described. In view of the results of Table 1, we thus decided to further explore the role of desulforedoxin as a potential electron donor to *Dg* SOR.

In order to perform this study, we had to modify our assay because of the high reactivity of desulforedoxin with the superoxide anion generated by the xanthine/xanthine oxidase system (3 times that observed in the case of rubredoxins, data not shown). In our modified assay, presented in Fig. 6 and described in the "Materials and methods," the reduction of desulforedoxin using sodium dithionite, characterized by the disappearance of the absorbance at 502 nm, was followed by addition of catalytic amounts of *Dg* SOR, resulting in no change in the residual absorbance. The superoxide-generating system was only added in the second part of the kinetics assay, and resulted in the oxidation of desulforedoxin, with a rate proportional to the amount of SOR added in the first part of the kinetics assay, in agreement with a direct electron transfer between the two proteins (Fig. 6).

In order to validate this new assay, electron transfer reactions between *Dg* rubredoxin and *Dg* SOR were performed using the two experimental procedures, and the results are presented in Fig. 7 (open circles and squares). As expected, the rubredoxin oxidation rate obtained using the new procedure was the same as that obtained from the difference of the rubredoxin oxidation rates, before and upon addition of the xanthine/xanthine oxidase system, determined using our classical kinetics assay. Comparison of the data confirmed that the k_{app} value calculated using the modified procedure, 32.0 ± 7.8 min^{-1} (Fig. 7, squares), was similar to that determined using our classical assay, 32.9 ± 4.2 min^{-1} (Fig. 7, open circles).

Figure 7 also shows the plot of the rates of desulforedoxin oxidation, upon addition of various amounts of *Dg* SOR (filled circles). The derivation of this curve allowed the direct calculation of the k_{app} value for the superoxide-mediated electron transfer reaction between desulforedoxin and SOR, 108.8 ± 12.0 min^{-1} (Table 1). Comparison of the two k_{app} values, for rubredoxin and desulforedoxin, derived from the plots of Fig. 7,

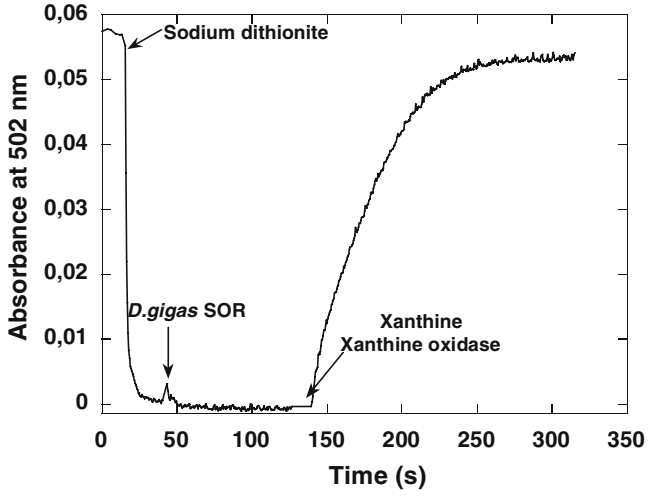

Fig. 6 Kinetics trace of superoxide-mediated electron transfer between *Dg* desulforedoxin and *Dg* SOR, measured at 502 nm. The assay was performed aerobically at 20 °C in a 1-ml quartz cuvette containing 9 μM desulforedoxin in 50 mM phosphate buffer, pH 7.8, as described in the "Materials and methods." After addition of sodium dithionite, the reduction of desulforedoxin was reflected by a decrease in the absorbance at 502 nm. After approximately 1 min, 0.07 μM *Dg* SOR was added to the cuvette, with no change in absorbance at 502 nm. Xanthine (0.5 mM) and xanthine oxidase (0.058 U ml^{-1}) were then added to the reaction mixture, in the presence of 150 U ml^{-1} catalase, resulting in the fast oxidation of desulforedoxin

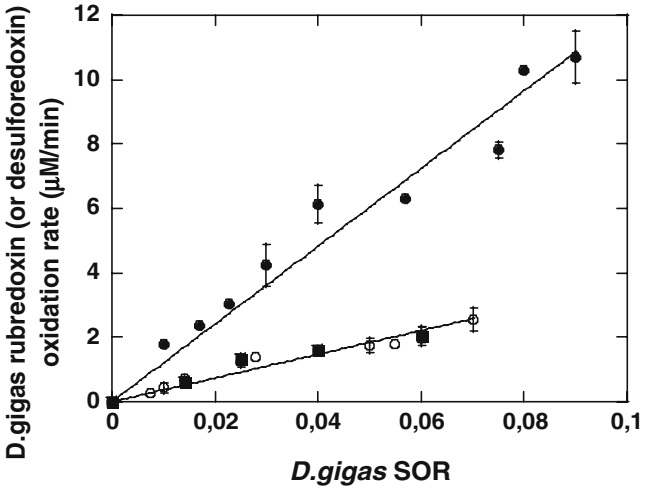

Fig. 7 Superoxide-mediated electron transfer from *Dg* rubredoxin (*open circles* and *squares*) and *Dg* desulforedoxin (*filled circles*) to *Dg* SOR. Experiments were performed using the assay in which different concentrations of oxidized *Dg* SOR were added before the superoxide-generating system (see Fig. 6 and the "Material and methods"). The specific desulforedoxin oxidation rates were derived from the linear part of the kinetics trace of Fig. 6 (*filled circles*). In order to allow the comparison of the data, similar experiments were performed using *Dg* rubredoxin as the electron donor for *Dg* SOR (*squares*). *Open circles* are the *Dg* rubredoxin oxidation rates to *Dg* SOR determined using the method described in the legend of Fig. 6, in which the enzyme was added last. All data points in the figure represent averages of triplicates or more determinations. Where not visible in the figure, the range bars lie within the diameter of the symbol

demonstrates that *Dg* desulforedoxin was able to transfer electrons more efficiently than *Dg* rubredoxin, which presents a k_{app} value of 31.8 ± 3.6 min^{-1} (Table 1, using values from the classical and the modified procedure). In view of these results, we propose that desulforedoxin is the physiological electron donor for SOR in *Dg*.

Discussion

In this work, we have presented kinetics studies of the superoxide-mediated electron transfer reactions between the three different classes of SORs described in the literature and their respective putative electron donor rubredoxins. The two-iron SOR from *Dv* belongs to class I [9, 16–18], SOR from *Dg* to belongs to class II [3, 24], and SOR from *Tp* was chosen as an example of class III [5, 8] (Fig. 1). All the possible combinations of the reactions between the three SORs and their homolog rubredoxins were systematically explored. Altogether, the results showed that the three rubredoxins were able to transfer electrons to the three different SORs (Tables 1, 2), at reasonable rates to be considered physiologically possible.

Development of activity assays of SORs had led to discrepancies in the literature, mainly because of the difficulties of assaying superoxide and of the myriad of redox reactions that can take place between compounds in the assay [2, 4, 5, 7, 24, 31, 55]. The first specific activity assay for SORs was proposed in Refs. [33, 46] and the activity of SOR was measured with a detection limit of around 50 nM. Interesting results were also obtained when pulse radiolysis was used to generate superoxide, but this method is very difficult to use as a routine assay in a laboratory [31].

The results presented here suggest that our experimental procedure could be used as an alternative in vitro activity assay for the different classes of SORs, after choosing a rubredoxin available in the laboratory, as already proposed by our group [32]. It is now currently admitted that SORs present very low or no SOD activity and that a good assay for SORs should be specific and allow a clear discrimination of the dismutation reaction from the reduction of superoxide catalyzed by SORs.

In our assay, addition of equivalent amounts of both SOR and SOD (Fig. 3, trace b) leads to an inhibition of the rubredoxin oxidation rate, because SOD can compete with SOR for reaction with the superoxide anion, with a similar virtually diffusion limited rate of 10^9 M^{-1} s^{-1} [7, 10, 29, 31]. However, when SOD only was added in an equivalent concentration, complete inhibition of rubredoxin reoxidation was observed (Fig. 3, trace c). Indeed, SOD, which, under our experimental conditions, was able to totally inhibit the flux of superoxide generated by the xanthine oxidase (Fig. 3, trace d), was nevertheless unable to receive electrons from rubredoxin at rates able to compete with the catalytic reduction of superoxide (10^9 M^{-1} s^{-1}) [7, 10, 29, 31]. Altogether, these results show unequivocally that our assay allows discrimination between a SOR and a SOD activity.

In addition, a modified hexacoordinated form of SOR, such as the ferrocyanide adduct produced upon oxidation of the enzyme using potassium ferricyanide [56], was shown to be unable to catalyze the superoxide-mediated oxidation of rubredoxin (Fig. 4). This shows that our experimental procedure can be used to measure SOR activity in vitro. However, in the absence of orthogonal data such as microarray assays or proteomics, it will be difficult, on the basis of these data alone, to discriminate in vivo between active and inactive forms of SORs.

Under our experimental conditions, we can assume there to be a steady-state concentration of superoxide, saturating concentration of rubredoxin, and less than saturating concentrations of SOR, so the rate-limiting step of the process must be the reaction of SOR with rubredoxin, knowing that superoxide has been shown to react with the active site of each of the three SORs studied with the virtually diffusion controlled rate of 10^9 M^{-1} s^{-1}[10, 19, 28–31].

Therefore, the different k_{app} values calculated for the different superoxide-mediated reactions (Tables 1, 2) cannot be attributed to a difference of reactivity of SORs with $O_2^{\bullet -}$, but should reflect the respective abilities of SOR to accept electrons from rubredoxins. As an example, class I *Dv* SOR and class II *Dg* SOR receive more specifically electrons from their potential physiological electron donor (Tables 1, 2) and these results could suggest a trend to a specific SOR/rubredoxin interaction.

However, *Tp* SOR was also able to receive electrons from *Dg* rubredoxin, with a rate of 213.4 ± 38.4 min^{-1}, as well as from desulforedoxin, another rubredoxin-type protein, with a k_{app} value of 156.0 ± 19.0 min^{-1}, rates that are physiologically acceptable (Table 1). Interestingly, the values reported for *Tp* SOR are much higher that those reported here for any of the other systems.

In the case of *Dg*, in addition to rubredoxin, this organism also expresses the gene coding for a small homodimeric non-heme iron protein called desulforedoxin [9, 21, 22, 54, 57]. The coexistence, in the same organism, of these two proteins has raised the question of a possible role of desulforedoxin in the electron transfer chain leading to the reduction of superoxide in *Dg*. In order to test the electron transfer capability of desulforedoxin, reactions between this protein and class II *Dg* SOR were studied.

We had to modify our classical kinetics assay, because we observed a high activity of desulforedoxin towards the superoxide anion, which cannot be explained only by the difference of midpoint potential between the two electron carriers [E^0(rubredoxin Fe^{3+}/Fe^{2+}) = +6 mV and E^0(desulforedoxin Fe^{3+}/Fe^{2+}) = −35 mV] [9, 22]. The only noticeable difference we found between the metal centers of these two proteins is the exposure to solvent and the presence of structural water molecules in the

vicinity (5 Å) of the iron center, implicated in the mediation of the electron transfer in desulforedoxin [51].

The superoxide-mediated electron transfer reaction between desulforedoxin and *Dg* SOR (k_{app} of 108.8 ± 12.0 min^{-1}) was found to be more efficient than that observed between rubredoxin and SOR isolated from the same organism (k_{app} of 31.8 ± 3.6 min^{-1}) (Fig. 7). These experiments bring, to our knowledge, the first kinetics evidence for desulforedoxin as a redox partner of *Dg* SOR, and suggest that desulforedoxin could be the physiological electron donor for SOR in the *Dg* species. However, the physiological signification of the coexistence of both rubredoxin and desulforedoxin, two potential electron donors, in the same organism remains to be answered.

In the case of the two-iron class I *Dv* SOR [9, 16–18] our results show unequivocally that the protein was able to receive electrons from the three rubredoxins under study. These results agree with previously published data which demonstrate that *Dv* rubredoxin is a competent proximal electron donor to *Dv* SOR [33, 34, 46]. In addition, the existence of a rubredoxin/SOR redox partnership is consistent with the cotranscription of their genes in *Dv* [16]. This fact suggests that the electron transfer rates determined between rubredoxin and *Dv* SOR (Table 2) could be physiologically relevant, even if lower that those determined for the other classes of SORs.

In the case of class I *Dv* SOR, it has been suggested that electron transfer can occur between center I located in the N-terminal domain, highly homologous (67%) with *Dg* desulforedoxin, and the neelaredoxin-like center II (Scheme 1, pathway 3–4), overcoming the need of rubredoxin to donate electrons to center II [2, 16, 45]. Indeed, as shown in the scheme, center I (+4 mV) is thermodynamically capable of reducing center II (+240 mV). Therefore, rubredoxin can act as an intermolecular electron donor, followed by an intramolecular process between center I and center II (Scheme 1, pathway 3–4).

Coulter et al. [33, 46] demonstrated that *Dv* rubredoxin catalyzes reduction of both centers I and II, but the reduction of center II was at least fourfold faster than that observed for center I. Besides, on the basis of redox potential and the solvent accessibility, center II should be reduced more efficiently than center I (Scheme 1, pathway 2). It has also been demonstrated that an engineered SOR lacking center I retains its catalytic activity and that rubredoxin is an efficient electron donor to center II [34], and that removal of center I has no influence on the rubredoxin/center II electron transfer rates [28, 34, 46]. In fact, iron–iron distances in class I SORs seem to be too large to enable efficient electron transfer (monomer, intrasubunit Fe–Fe 22 Å; dimer, intersubunit Fe–Fe 32 Å) [14, 58–60].

Under our experimental conditions, it would be expected that center II in the gray form of *Dv* SOR (fully oxidized) would be immediately reduced by rubredoxin (becoming the pink form) and would have an identical turnover to the *Dv* SOR pink form; however, comparison of the k_{app} values obtained for the pink and gray forms of *Dv* SOR have shown that, under our experimental conditions, the electron transfer reaction seems to be more efficient between rubredoxin and the pink form (oxidized center I, reduced center II) than between rubredoxin and the fully oxidized gray form (Table 2).

Although these data alone do not allow a conclusion to be drawn for a possible role of center I, we propose that the slower electron transfer rates observed for the gray form of SOR could imply a molecular rearrangement associated with the reduction of center I that changes the rate of electron transfer from rubredoxin to center II. Actually, in bacterial enzymes containing more than one domain, such as bacterial cytochrome *c* peroxidase and nitrite reductase cytochrome cd_1, it has been observed that reduction of the redox center in one of the domains implies a structural change in the protein [62–65]. Therefore, similar behavior cannot be ruled out for this enzyme and further experiments are currently in progress in our laboratory to test this hypothesis.

Comparison of the data in Tables 1 and 2 also revealed different orders of magnitude concerning the superoxide-mediated electron transfer reactions between the different rubredoxin-like proteins and their homologs SORs. Indeed, *Tp*, usually classified as a microaerophile, is able to receive electrons from the different rubredoxin-like proteins, with high k_{app} values varying from 156 to 213 min^{-1}, with the notable exception of *Dv* rubredoxin. As already described, superoxide reacts with the active site of the three SORs studied with the same rate of 10^9 M^{-1} s^{-1} [10, 19, 28–31], and therefore our results could suggest that *Tp* needs a faster electron transfer system to be able to deal with the relatively high concentrations of oxygen encountered during the

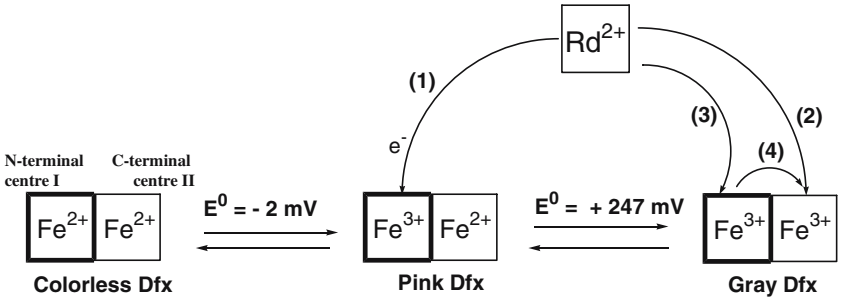

Scheme 1 The different possible electron transfer pathways implicated in the reaction between *Desulfovibrio vulgaris* (*Dv*) rubredoxin and two forms of the *Dv* two-iron superoxide reductase (pink and gray forms)

dissemination of the spirochete into the tissues, lowering the superoxide concentration to nonlethal levels.

Inversely, aerotolerant organisms such as *Dv* and *Dg* are supposed to be exposed more briefly to oxygen and at much lower concentrations, as reflected in the lower k_{app} values observed. In addition, *Dv*, which apparently possesses the lower SOR activity, was shown to express the gene for a periplasmic SOD [44]. These differences could reveal an extraordinary faculty of these organisms to deal with the oxidative stress, and we suggest that the efficiency of the superoxide-mediated electron transfer reactions may be related to an adaptation of the bacteria to environmental conditions.

Acknowledgements This work was supported by the Fundação para a Ciência e Tecnologia (grants SFRH/BPD/12003/2003 and SFRH/BDP/14067/2003).

References

1. Abreu IA, Saraiva LM, Carita J, Huber H, Stetter KO, Cabelli D, Teixeira M (2000) Mol Microbiol 38(2):322–334
2. Ascenso C, Rusnak F, Cabrito I, Lima MJ, Naylor S, Moura I, Moura JJ (2000) J Biol Inorg Chem 5(6):720–729
3. Chen L, Sharma P, Le Gall J, Mariano AM, Teixeira M, Xavier AV (1994) Eur J Biochem 226(2):613–618
4. Jenney FE Jr, Verhagen MF, Cui X, Adams MW (1999) Science 286(5438):306–309
5. Jovanovic T, Ascenso C, Hazlett KR, Sikkink R, Krebs C, Litwiller R, Benson LM, Moura I, Moura JJG, Radolf JD, Huynh BH, Naylor S, Rusnak F (2000) J Biol Chem 275(37):28439–28448
6. Kurtz DM Jr (2004) Acc Chem Res 37(11):902–908
7. Lombard M, Fontecave M, Touati D, Niviere V (2000) J Biol Chem 275(1):115–121
8. Lombard M, Touati D, Fontecave M, Nivière V (2000) J Biol Chem 275(35):27021–27026
9. Moura I, Tavares P, Moura JJ, Ravi N, Huynh BH, Liu MY, LeGall J (1990) J Biol Chem 265(35):21596–21602
10. Niviere V, Fontecave M (2004) J Biol Inorg Chem 9(2):119–123
11. Tavares P, Ravi N, Moura JJG, LeGall J, Huang YH, Crouse BR, Johnson MK, Huynh BH, Moura I (1994) J Biol Chem 269(14):10504–10510
12. Rusnak F, Ascenso C, Moura I, Moura JJ (2002) Methods Enzymol 349:243–258
13. Clay MD, Jenney FE Jr, Hagedoorn PL, George GN, Adams MW, Johnson MK (2002) J Am Chem Soc 124(5):788–805
14. Coelho AV, Matias PM, Carrondo MA, Tavares P, Moura JJ, Moura I, Fulop V, Hajdu J, Le Gall J (1996) Protein Sci 5(6):1189–1191
15. Yeh AP, Hu Y, Jenney FE Jr, Adams MW, Rees DC (2000) Biochemistry 39(10):2499–2508
16. Brumlik MJ, Voordouw G (1989) J Bacteriol 171(9):4996–5004
17. Devreese B, Tavares P, Lampreia J, Van Damme N, Le Gall J, Moura JJ, Van Beeumen J, Moura I (1996) FEBS Lett 385(3):138–142
18. Verhagen MF, Voorhorst WG, Kolkman JA, Wolbert RB, Hagen WR (1993) FEBS Lett 336(1):13–18
19. Lombard M, Houée-Levin C, Touati D, Fontecave M, Nivière V (2001) Biochemistry 40(16):5032–5040
20. Pianzzola MJ, Soubes M, Touati D (1996) J Bacteriol 178(23):6736–6742
21. Moura I, Bruschi M, Le Gall J, Moura JJ, Xavier AV (1977) Biochem Biophys Res Commun 75(4):1037–1044
22. Moura I, Huynh BH, Hausinger RP, Le Gall J, Xavier AV, Munck E (1980) J Biol Chem 255(6):2493–2498
23. Moura JJG, Goodfellow BJ, Romao MJ, Rusnak F, Moura I (1996) Comments Inorg Chem 19(1):47–66
24. Silva G, Oliveira S, Gomes CM, Pacheco I, Liu MY, Xavier AV, Teixeira M, Legall J, Rodrigues-Pousada C (1999) Eur J Biochem 259(1–2):235–243
25. Klenk HP, Clayton RA, Tomb JF, White O, Nelson KE, Ketchum KA, Dodson RJ, Gwinn M, Hickey EK, Peterson JD, Richardson DL, Kerlavage AR, Graham DE, Kyrpides NC, Fleischmann RD, Quackenbush J, Lee NH, Sutton GG, Gill S, Kirkness EF, Dougherty BA, McKenney K, Adams MD, Loftus B, Venter JC et al (1997) Nature 390(6658):364–370
26. Bult CJ, White O, Olsen GJ, Zhou L, Fleischmann RD, Sutton GG, Blake JA, FitzGerald LM, Clayton RA, Gocayne JD, Kerlavage AR, Dougherty BA, Tomb JF, Adams MD, Reich CI, Overbeek R, Kirkness EF, Weinstock KG, Merrick JM, Glodek A, Scott JL, Geoghagen NS, Venter JC (1996) Science 273(5278):1058–1073
27. Fraser CM, Norris SJ, Weinstock GM, White O, Sutton GG, Dodson R, Gwinn M, Hickey EK, Clayton R, Ketchum KA, Sodergren E, Hardham JM, McLeod MP, Salzberg S, Peterson J, Khalak H, Richardson D, Howell JK, Chidambaram M, Utterback T, McDonald L, Artiach P, Bowman C, Cotton MD, Venter JC et al (1998) Science 281(5375):375–388
28. Abreu IA, Saraiva LM, Soares CM, Teixeira M, Cabelli DE (2001) J Biol Chem 276(42):38995–39001
29. Coulter E, Emerson J, Kurtz D, Cabelli D (2000) J Am Chem Soc 122:11555–11556
30. Emerson JP, Coulter ED, Cabelli DE, Phillips RS, Kurtz DM Jr (2002) Biochemistry 41(13):4348–4357
31. Niviere V, Lombard M, Fontecave M, Houee-Levin C (2001) FEBS Lett 497(2–3):171–173
32. Auchere F, Sikkink R, Cordas C, Raleiras P, Tavares P, Moura I, Moura JJ (2004) J Biol Inorg Chem 9(7):839–849
33. Coulter ED, Kurtz DM Jr (2001) Arch Biochem Biophys 394(1):76–86
34. Emerson JP, Cabelli DE, Kurtz DM Jr (2003) Proc Natl Acad Sci USA 100(7):3802–3807
35. Grunden AM, Jenney FE Jr, Ma K, Ji M, Weinberg MV, Adams MW (2005) Appl Environ Microbiol 71(3):1522–1530
36. Rodrigues JV, Abreu IA, Saraiva LM, Teixeira M (2005) Biochem Biophys Res Commun 329(4):1300–1305
37. Lovenberg W, Sobel BE (1965) Proc Natl Acad Sci USA 54(1):193–199
38. Bachmayer H, Yasunobu KT (1967) Biochem Biophys Res Commun 26(4):435–440
39. Eidsness MK, Richie KA, Burden AE, Kurtz DM Jr, Scott RA (1997) Biochemistry 36(34):10406–10413
40. Lovenberg W, Williams WM (1969) Biochemistry 8(1):141–148
41. Peisach J, Blumberg WE, Lode ET, Coon MJ (1971) J Biol Chem 246(19):5877–5881
42. Sieker LC, Stenkamp RE, LeGall J (1994) Methods Enzymol 243:203–216
43. Das A, Coulter E, Kurtz D, Ljungdahl L (2001) J Bacteriol 183:1560–1567
44. Lumppio HL, Shenvi NV, Summers AO, Voordouw G, Kurtz DM Jr (2001) J Bacteriol 183(1):101–108
45. Silva G, LeGall J, Xavier AV, Teixeira M, Rodrigues-Pousada C (2001) J Bacteriol 183(15):4413–4420
46. Emerson JP, Coulter ED, Phillips RS, Kurtz DM Jr (2003) J Biol Chem 278(41):39662–39668
47. Czaja C, Litwiller R, Tomlinson AJ, Naylor S, Tavares P, LeGall J, Moura JJG, Moura I, Rusnak F (1995) J Biol Chem 270(35):20273–20277
48. Creutz C, Sutin N (1973) Proc Natl Acad Sci USA 70(6):1701–1703
49. Bruschi M, Le Gall J (1972) Biochim Biophys Acta 263(2):279–282
50. Le Gall J (1968) Ann Inst Pasteur (Paris) 114(1):109–115
51. Archer M, Huber R, Tavares P, Moura I, Moura JJ, Carrondo MA, Sieker LC, LeGall J, Romao MJ (1995) J Mol Biol 251(5):690–702

52. McCord JM, Fridovich I (1969) J Biol Chem 244(22):6049–6055
53. Fridovich I (1970) J Biol Chem 245(16):4053–4057
54. Bruschi M, Moura I, Le Gall J, Xavier AV, Sieker LC, Couchoud P (1979) Biochem Biophys Res Commun 90(2):596–605
55. Romao CV, Liu MY, Le Gall J, Gomes CM, Braga V, Pacheco I, Xavier AV, Teixeira M (1999) Eur J Biochem 261(2):438–443
56. Auchère F, Raleiras P, Benson L, Venyaminov SY, Tavares P, Moura JJG, Moura I, Rusnak F (2003) Inorg Chem 42(4):938–940
57. Brumlik MJ, Leroy G, Bruschi M, Voordouw G (1990) J Bacteriol 172(12):7289–7292
58. Kurtz DM Jr, Coulter ED (2002) J Biol Inorg Chem 7(6):653–658
59. Liochev SI, Fridovich I (1997) J Biol Chem 272(41):25573–25575
60. Page CC, Moser CC, Chen X, Dutton PL (1999) Nature 402(6757):47–52
61. Kopp J, Schwede T (2004) Nucleic Acids Res 32:D230–D234
62. Dias JM, Alves T, Bonifacio C, Pereira AS, Trincao J, Bourgeois D, Moura I, Romao MJ (2004) Structure (Camb) 12(6):961–973
63. Shimizu H, Schuller DJ, Lanzilotta WN, Sundaramoorthy M, Arciero DM, Hooper AB, Poulos TL (2001) Biochemistry 40(45):13483–13490
64. Allen JW, Watmough NJ, Ferguson SJ (2000) Nat Struct Biol 7(10):885–888
65. Gordon EH, Sjogren T, Lofqvist M, Richter CD, Allen JW, Higham CW, Hajdu J, Fulop V, Ferguson SJ (2003) J Biol Chem 278(14):11773–11781